The Sturge-Weber syndrome: comparison of MR and CT characteristics.

J J Wasenko, S A Rosenbloom, P M Duchesneau, C F Lanzieri and M A Weinstein

AJNR Am J Neuroradiol 1990, 11 (1) 131-134
http://www.ajnr.org/content/11/1/131

The Sturge-Weber Syndrome:
Comparison of MR and CT Characteristics

John J .Wasenko[1]
Scott A. Rosenbloom
Paul M. Duchesneau
Charles F. Lanzieri
Meredith A. Weinstein

Four patients with Sturge-Weber syndrome were evaluated with CT and MR. MR demonstrated the characteristic features of the disease: cerebral atrophy (four patients), ipsilateral bone and sinus hypertrophy (three), ocular findings (one), intracranial calcification (four), prominent deep venous system (three), and enlarged choroid plexus (two). CT demonstrated the following: cerebral atrophy (four), ipsilateral bone and sinus hypertrophy (three), calcification (four), gyral enhancement (two), prominent deep venous system (two), and enlarged choroid plexuses (three).

The features of Sturge-Weber syndrome were visualized equally well with MR and CT with the exception of intracranial calcification. Conventional spin-echo MR revealed fewer calcifications, and those visualized appeared smaller than with CT. Gradient-echo acquisition sequences were more effective in the detection of intracranial calcification.

***AJNR* 11:131–134, January/February 1990**

Sturge-Weber syndrome is one of the neurocutaneous syndromes and was first described by Sturge in 1879 [1]. Weber demonstrated the characteristic intracranial calcifications in 1929 [2]. It is a rare, nonfamilial disease that is characterized by the following features: port-wine stain (nevus flammeus), leptomeningeal angiomatosis, choroidal angioma, buphthalmos, intracranial calcification, cerebral atrophy, mental retardation, glaucoma, seizures, hemiparesis, and hemiatrophy [3].

Prior to the advent of CT, the diagnosis of Sturge-Weber syndrome was made by plain skull films and angiography. CT greatly aided the diagnosis of the disease [4–15], and several reports have described its MR appearance [16–18]. A review of these reports suggests that MR better demonstrates the vascular anomalies while CT is more sensitive for the detection of calcification [19]. To date, a comparative study of CT and MR in the evaluation of Sturge-Weber syndrome has not been performed, and this was the purpose of our study.

Materials and Methods

Four patients with Sturge-Weber syndrome were evaluated with CT and MR imaging. Clinically, mental retardation, seizures, and port-wine nevus were present in four patients; one patient had port-wine nevi bilaterally, and one had buphthalmos. Two patients were female and two were male; their ages ranged from 7 to 16 years. CT was performed on a Picker 1200 SX scanner. Unenhanced scans in the axial plane were performed in all four patients and enhanced scans were performed in three of these. IV Hypaque meglumine 60% at a dose of 1 ml/kg was used.

MR was performed on a General Electric 1.5 T unit in one patient and on Technicare 0.6 T and 1.5 T superconducting magnets in one and two patients, respectively. Imaging parameters for the General Electric unit were as follows: matrix size 256 × 192, field of view 24 cm, and an interleaved slice thickness of 5 mm. Sagittal T1-weighted, 500/30/1 (TR/TE excitations), axial spin-density-weighted, 2000/30, and T2-weighted, 2000/80, images were obtained. Coronal T2-weighted images were obtained in one patient. Parameters for the

Received March 24, 1989; revision requested May 2, 1989; revision received June 22, 1989; accepted July 3, 1989.

[1] All authors: Division of Radiology, Cleveland Clinic Foundation, 9500 Euclid Ave., Cleveland, OH 44195-5103. Address reprint requests to S. A. Rosenbloom.

0195–6108/90/1101–0131

Technicare units were as follows: matrix size 192 × 192, field of view 25.6 cm, and slice thickness 6.5 mm with a 25% gap. Sagittal T1-weighted, 500/32/2, axial spin-density-weighted, 2010/32, and T2-weighted, 2010/120, images were obtained. T1-weighted axial images were obtained in one patient. Gradient-echo (GRE) sequences were performed in two patients, with parameters of 200/13–30/10° (TR/TE/flip angle) to maximize T2* contrast.

Results

The CT and MR findings for all cases are summarized in Table 1.

Atrophy/hypertrophy. Right parietooccipital atrophy was present in one patient. Two patients demonstrated right frontoparietal atrophy; one of these patients also had left parietal atrophy. The remaining patient had left frontoparietooccipital atrophy. Compensatory hypertrophy of the frontal bone and frontal sinus was present on the side of hemispheric atrophy in three of four patients. The hemispheric atrophy and bone hypertrophy were well demonstrated by both CT and MR (Fig. 1).

Ocular findings. Buphthalmos (congenital enlarged globe and glaucoma) was present in one patient. The left globe was enlarged and demonstrated retinal or choroidal detachment. MR revealed lens-shaped areas of increased signal, consistent with subacute hemorrhage, in both the medial and lateral aspects of the globe on all pulse sequences. The orbits were not visualized with CT in this patient.

Intracranial calcification. CT identified calcification on the side of atrophy in all patients. In addition, bilateral calcification was present in the patient with bilateral atrophy. Conventional spin-echo MR identified the calcifications in three of four patients. These appeared as areas of decreased signal intensity on the spin-density and T2-weighted images (Fig. 2). However, fewer calcifications were identified with MR and they appeared smaller than on CT. In one patient, no calcifications were identified even though they were large and multiple on CT. GRE sequences were performed in this patient and in a second patient. All calcifications present on the CT examinations were identified on GRE sequences as areas of decreased signal intensity. Also, the size of the calcifications was larger than that noted with conventional spin-echo sequences and approximately equal in size to that noted on CT (Fig. 3).

Gyral enhancement. Contrast-enhanced CT was performed in three of four patients. Gyral enhancement was present on the side of atrophy in two of these three patients. Gadolinium-enhanced MR was not performed.

Venous system. A prominent deep venous system was identified on the side of atrophy in two patients with both MR and contrast-enhanced CT; in case 1 it was demonstrated with MR only. These patients demonstrated prominent deep medullary and subependymal veins. One of these patients had bilateral atrophy and calcification as well as prominent deep medullary, subependymal, and internal cerebral veins bilaterally (Fig. 4). Unenhanced CT did not show these abnormalities.

TABLE 1: Summary of CT and MR Findings in Patients with Sturge-Weber Syndrome

Case No.	Cerebral Atrophy		Bone/ Sinus Hypertrophy		Ocular Findings		Intracranial Calcification		Gyral Enhancement		Venous System		Choroid Plexus	
	CT	MR	CT	MR	CT	MR	CT	MR	CT	MR	CT	MR	CT	MR
1	+	+	+	+	NI	−	++	+	−	NS	−	+	+	+
2	+	+	−	−	−	−	++	+	+	NS	+	+	+	−
3	+	+	+	+	NI	+	++	GRE	+	NS	+	+	+	+
4	+	+	+	+	NI	−	++	+	NS	NS	NS	−	−	−

Note.—+ = finding present, − = finding absent, ++ = finding better visualized with one method than the other, NI = area not imaged, GRE = finding seen with GRE sequence, NS = unenhanced study, finding not seen.

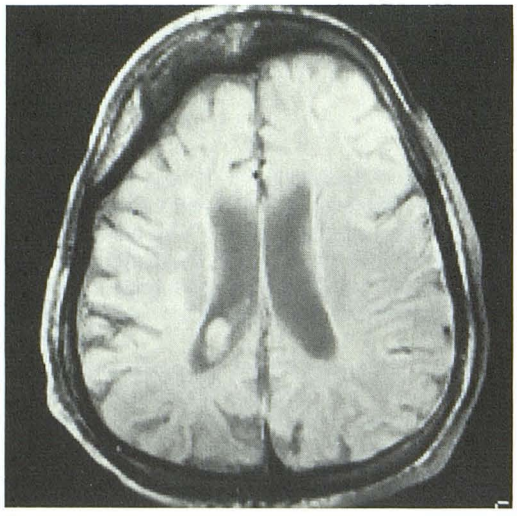

1

2

Fig. 1.—Spin-density-weighted image (2010/32) shows right hemispheric atrophy with compensatory bone hypertrophy. Enlarged choroid plexus, representing an angiomatous malformation, is present in right lateral ventricle.

Fig. 2.—Gyral calcifications in right parietal lobe appear as areas of decreased signal intensity on this T2-weighted image (2010/120).

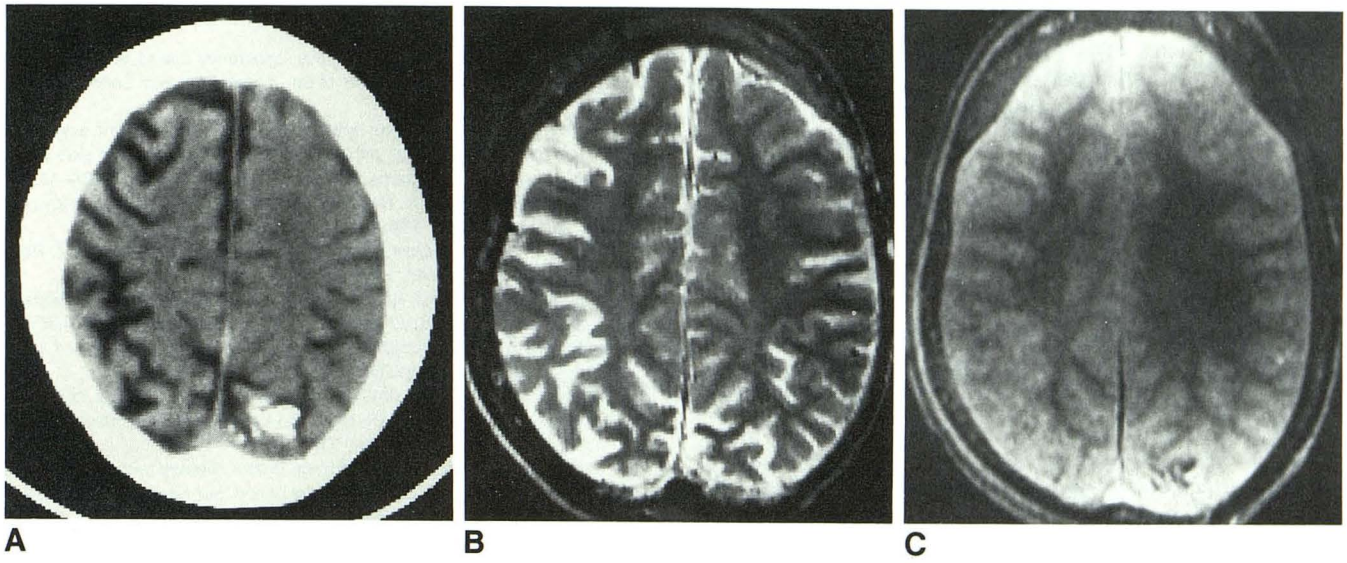

Fig. 3.—*A*, Unenhanced CT scan shows bilateral hemispheric atrophy and left parietal gyral calcifications. *B*, T2-weighted image (2010/120) at same level shows bilateral hemispheric atrophy but fails to demonstrate gyral calcification. *C*, Gradient-echo sequence (200/13/10°) reveals that gyral calcification is vizualized because of its magnetic susceptibility.

Choroid plexus. The size of the choroid plexus was determined by obtaining the transverse diameter of the glomus of the choroid plexus. The diameters of the choroid plexus on contrast-enhanced CT were 10 mm (case 1), 8 mm (case 2), and 7 and 9 mm (case 3). A large, prominently enhancing choroid plexus was identified on the side of atrophy in three patients who had contrast-enhanced CT. In the patient with bilateral atrophy, this was present in both lateral ventricles. A prominent choroid plexus was not identified in the patient studied with unenhanced CT. MR demonstrated a prominent choroid plexus in two patients (Fig. 1). The signal intensity of the choroid was identical to that of gray matter on all pulse sequences.

White matter myelination. Normal myelination was present in all patients.

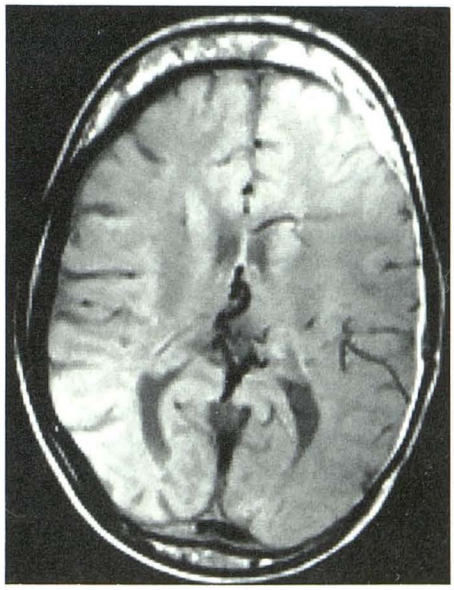

Fig. 4.—Same patient as in Fig. 3. Spin-density-weighted image (2010/32) shows curvilinear areas of decreased signal representing enlarged internal cerebral, deep medullary, and subependymal veins.

Discussion

A diagnosis of Sturge-Weber syndrome is readily made with CT. Several reports have described features of the syndrome on MR. Specifically, accelerated myelination has been noted in the abnormal hemisphere in infants; however, the mechanism is unknown [16]. Accelerated myelination was not present in any patient in this report. In addition, cerebral atrophy, most common in the parietooccipital region, is also well demonstrated with MR [18, 19], as is compensatory frontal bone and sinus hypertrophy.

Buphthalmos (congenital enlarged globe and glaucoma) and choroidal angiomas may be seen in Sturge-Weber syndrome. One patient with congenital glaucoma demonstrated a large globe with retinal or choroidal detachment.

A prominent choroid plexus resulting from angiomatous malformation has been reported to be a common finding in Sturge-Weber syndrome [17]. The size of the glomus of the choroid plexus on contrast-enhanced CT in normal patients ages 6–10 and 11–15 years is 2.5 and 3.5 mm, respectively [17]. The average size of the abnormal choroid plexuses in this study of Sturge-Weber syndrome was 8 mm. Three of our four patients had enlarged choroid plexuses, which enhanced with IV contrast. MR revealed prominent choroid plexuses in two patients. An enlarged choroid plexus visualized with CT in one patient but not demonstrated with MR was most likely due to partial volume averaging with CSF. The signal intensity of the abnormal choroid plexus was isointense with gray matter on all pulse sequences rather than increased in signal intensity on T2-weighted images as previously noted [17].

The basic venous abnormality in this syndrome is a lack of superficial cortical veins overlying the area of cerebral atrophy.

Enlarged internal cerebral, basal Rosenthal, deep medullary, and subependymal veins may be seen [20]. MR and contrast-enhanced CT demonstrated a prominent deep venous system in two patients; however, a lack of superficial cortical veins was not demonstrated in either patient. In a third patient, a prominent deep venous system was demonstrated with MR only. Although a prominent vein of Rosenthal is a common abnormality [20], this was not visualized with MR or CT in our series.

The intracranial calcifications were not as well visualized with conventional spin-echo MR as with CT. MR demonstrated fewer calcifications and those visualized appeared smaller in size compared with CT. Calcification readily identified with CT may not be visualized with MR if small [21]. When identified, the calcifications appeared as areas of decreased signal intensity on spin-density and T2-weighted images. GRE imaging has been shown to reveal intracranial calcification as effectively as CT [22]. In this technique, the magnetic susceptibility of certain materials such as calcification creates local magnetic field gradients and results in increased T2 relaxation rates. This finding is nonspecific, however, and may also be caused by deoxyhemoglobin, hemosiderin, or interfaces of normal tissues with markedly different susceptibilities [23]. GRE sequences performed in two patients readily demonstrated the calcifications noted on CT. In case 3, the calcifications were slightly smaller than on CT, which was probably caused by the short TE used in the GRE sequence. Longer TEs are more sensitive to magnetic susceptibility and would more accurately display the true size of the calcifications. GRE sequences with longer TEs were performed but were severely degraded by noise.

Gadolinium-enhanced MR was not performed in this study. Presumably, this would demonstrate gyral and choroid plexus enhancement as well as enhancement of prominent deep veins.

MR thus demonstrates the manifestations of Sturge-Weber syndrome as effectively as CT if GRE imaging is included. Vascular anomalies are well visualized with MR without the use of IV contrast material. Intracranial calcification is better visualized with CT than with conventional spin-echo MR, but GRE imaging demonstrates calcification as effectively as CT does.

ACKNOWLEDGMENT

We thank Ellen Holly for her help in the preparation of this manuscript.

REFERENCES

1. Sturge WA. A case of partial epilepsy, apparently due to lesion of one of the vasomotor centers of the brain. *Trans Clin Soc Lond* **1879**;12: 162–167
2. Weber FP. Right sided hemi-hypertrophy resulting from right sided congenital spastic hemiplegia, with a morbid condition of the left side of the brain revealed by radiograms. *J Neurol Psychopathol* **1922**;3:134–139
3. Adams JH, Corellis JAN, Duchen LW. *Greenfield's neuropathology*, 4th ed. New York: Wiley, **1986**:431
4. New PFJ, Scott WR. *Computed tomography of the brain and orbit*. Baltimore: Williams & Wilkins, **1975**:421–423
5. Boltshauser E, Wilson J, Hoare RD. Sturge-Weber syndrome with bilateral intracranial calcification. *J Neurol Neurosurg Pysch* **1976**;39:429–435
6. Harwood-Nash DC. Congenital cranio-cerebral abnormalities and computed tomography. *Semin Roentgenol* **1977**;XII:39–51
7. Enzmann DR, Hayward RW, Norman D, Dunn RP. Cranial computed tomographic scan appearance of Sturge-Weber disease: unusual presentation. *Radiology* **1977**;122:721–724
8. Kitahara T, Maki Y. A case of Sturge-Weber disease with epilepsy and intracranial calcification at the neonatal period. *Eur Neurol* **1978**;17:8–12
9. Maki Y, Semba A. Computed tomography of Sturge-Weber disease. *Child's Brain* **1979**;5:51–61
10. Weisberg LA. Computed tomography in the diagnosis of intracranial vascular malformations. *J Comput Tomogr* **1979**;3:125–132
11. Welch K, Naheedy MH, Abroms IF, Strand RD. Computed tomography of Sturge-Weber syndrome in infants. *J Comput Assist Tomogr* **1980**;4: 33–36
12. Segall HD, Ahmadi J, McComb JG, Zee CS, Becker TS, Han JS. Computed tomographic observations pertinent to intracranial venous thrombotic and occlusive disease in childhood. *Radiology* **1982**;143:441–449
13. Ambrosetto P, Ambrosetto G, Michelucci R, Bacci A. Sturge-Weber syndrome without port-wine facial nevus: Report of 2 case studies by CT. *Child's Brain* **1983**;10:387–392
14. Gardeur D, Palmieri A, Mashaly R. Cranial computed tomography in the phakomatoses. *Neuroradiology* **1983**;25:293–304
15. Wagner EJ, Rao KCVG, Knipp HC. CT-angiographic correlation in Sturge-Weber syndrome. *J Comput Tomogr* **1981**;5:324–326
16. Jacoby CG, Yuh WTC, Afifi AK, Bell WE, Schelper RL, Sato Y. Accelerated myelination in early Sturge-Weber syndrome demonstrated by MR imaging. *J Comput Assist Tomogr* **1987**;11:226–231
17. Stimac GK, Soloman MA, Newton TH. CT and MR of angiomatous malformations of the choroid plexus in patients with Sturge-Weber disease. *AJNR* **1986**;7:623–627
18. Brant-Zawadzki M, Norman D. Magnetic resonance imaging of the central nervous system. New York: Raven, **1987**:150
19. Bilaniuk LT, Zimmerman RA, Hochman M, et al. MR of Sturge-Weber syndrome (abstr). *AJNR* **1987**;8:945
20. Bentson JR, Wilson GH, Newton TH. Cerebral venous drainage pattern of the Sturge-Weber syndrome. *Radiology* **1971**;101:111–118
21. Holland BA, Kucharczyk W, Brant-Zawadzki M, Norman D, Haas DK, Harper PS. MR of calcified intracranial lesions. *Radiology* **1985**;157: 353–356
22. Atlas SW, Grossman RI, Hackney DB, et al. Calcified intracranial lesions: detection with gradient-echo-acquisition rapid MR imaging. *AJNR* **1988**;9:253–259, *AJR* **1988**;150:1383–1389
23. Edelman RR, Johnson R, Buxton R, et al. MR of hemorrhage: a new approach. *AJNR* **1986**;7:751–756